Heaven's Light is Our Guide

DEPARTMENT OF ELECTRONICS & TELECOMMUNICATION ENGINEERING
RAJSHAHI UNIVERSITY OF ENGINEERING & TECHNOLOGY, BANGLADESH

Metasurface-Based Ultra-Wideband (UWB) Solar Absorber at UV to SWIR Region Using Complex Metal Structure.

Author
Musabbir Ul Islam
Roll No. 1904048
Department of Electronics & Telecommunication Engineering
Rajshahi University of Engineering & Technology

Supervised by
Dr. Md Rabiul Hasan
Associate Professor
Department of Electronics & Telecommunication Engineering
Rajshahi University of Engineering & Technology

ACKNOWLEDGEMENT

With profound gratitude and unwavering belief in divine grace, I acknowledge the Almighty's guidance throughout my thesis journey. Without His benevolence, this task would have been insurmountable. May His wisdom continue to lead us.

In this endeavor, I am immensely indebted to the esteemed **Dr. Md Rabiul Hasan**, Associate Professor, Department of Electronics & Telecommunication Engineering, Rajshahi University of Engineering & Technology, Rajshahi. His unwavering support and invaluable assistance throughout this study have been instrumental in its successful completion. At every step, his wise counsel and encouragement motivated me to strive for excellence and evolve into an independent researcher. His compassion and generosity served as a source of solace during times of mental strain. I consider myself incredibly fortunate to have him as my supervisor, and his inspiration has been the driving force behind this thesis.

My sincere gratitude extends to the entire faculty, whose precious time, expertise, and efforts have created an environment conducive to academic research. Their dedication to nurturing our intellect and fostering our growth is deeply appreciated.

Finally, I extend my heartfelt appreciation to my beloved parents, whose unwavering love and unwavering support have been the pillars of strength throughout my academic journey.

June 29, 2025 Musabbir Ul Islam

RUET, Rajshahi

Heaven's Light is Our Guide

CERTIFICATE

This is to certify that this thesis report entitled ***"Metasurface-Based Ultra-Wideband (UWB) Solar Absorber at UV to SWIR Region Using Complex Metal Structure."*** *has been submitted by* ***Musabbir Ul Islam, Roll:1904048*** *in partial fulfillment of the requirement for the award of the degree of Bachelor of Science in Department of Electronics & Telecommunication Engineering of Rajshahi University of Engineering & Technology is a record of the candidates own work carried out by him under my supervision. This thesis has not been submitted for the award of any other degree.*

Supervisor

_____

Dr. Md Rabiul Hasan
Associate Professor
Department of Electronics & Telecommunication Engineering
Rajshahi University of Engineering & Technology
Rajshahi-6204

External Examiner

_____

Sharaf Tasnim
Assistant Professor
Department of Electronics & Telecommunication Engineering
Rajshahi University of Engineering & Technology
Rajshahi-6204

Head of the Department

_____

Dr Mst. Fateha Samad
Professor
Department of Electronics & Telecommunication Engineering
Rajshahi University of Engineering & Technology
Rajshahi-6204

ABSTRACT

An ultra-wide band (UWB) metasurface solar absorber structure covering the ultraviolet to short-wave infrared (SWIR) wavelength region is presented in this thesis. The material constituting the metasurface absorber is a refractory metal, which can work under high-temperature conditions and complex electromagnetic environments (like solar radiation). This work achieved more than 90% absorption up to 2800 nm wavelength and got more than 80% absorption for up to 3500 nm wavelength, hence covering an ultra-wide band solar light. In the spectrum of 300 nm to 2800 nm, the average absorption was 95.61%, and in the spectrum of 300 nm to 3500 nm wavelength, the average absorption was 93.47%. Moreover, the absorption spectrum is not sensitive to polarization. The investigation continued for different oblique incidences, and the investigation found a 30° incidence angle to be the most convenient angle of light propagation. This book proposes a four-layer model for high absorption of solar light. A bottom metal layer (gold/aluminum) works as a good reflector, which further reflects the light that is not wholly absorbed and reflects it back to the titanium layer again, where it is absorbed. The proposed absorber model in this book had great prospects in the field of thermal electronic equipment and solar power generation.

Keywords: Metasurface, solar absorber, UWB, numerical analysis, refractory metal, absorption spectrum.

CONTENTS

LIST OF TABLES

LIST OF FIGURES

Chapter 1

Introduction

1.1 Introduction

A solar absorber is a substance or construction made expressly to efficiently absorb incident solar radiation and transform it into another useful energy source, usually heat or electricity [2][3]. In both photovoltaic and photothermal systems, solar absorbers are crucial parts. The absorber transforms absorbed sunlight into thermal energy that can be used directly or to power a heat engine in solar thermal applications like solar water heaters and concentrated solar power (CSP) plants [4].

A solar absorber's spectral absorptance determines how effective it is; in order to reduce energy loss, it should ideally have low emissivity in the thermal infrared region and high absorptivity (near unity) across the solar spectrum [5]. Creating a structure or material that effectively absorbs a wide range of wavelengths, particularly beyond the ultraviolet spectrum into the near-infrared and short-wave infrared regions [6], is critical to improving the total solar energy conversion efficiency.

The two-dimensional (2D) analogous of a metamaterial is a metasurface, which is an engineered structure made up of subwavelength elements (meta-atoms) arranged in a periodic or quasi-periodic pattern [7]. The geometry and spatial arrangement of these artificial structures determine the behavior of metasurfaces, in contrast to bulk materials whose optical characteristics are determined by atomic structure [8]. Unprecedented control over the polarization, absorption, and propagation of electromagnetic waves is made possible by metasurfaces. Metasurfaces are employed in solar absorbers to improve light-matter interaction via Fabry-Pérot-type interference, electric and magnetic dipole resonances, and localized surface plasmon resonances

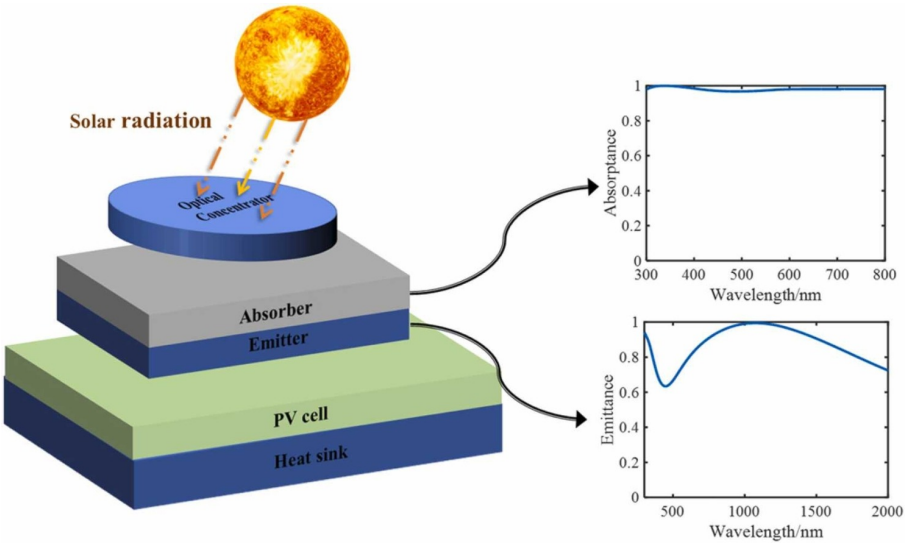

Figure 1.1: Basic principle demonstration of solar absorbers [1].

(LSPRs) [9][10]. Ultra-broadband and near-unity absorption can result from engineering these effects to overlap over a wide spectral range.

The spectral bandwidth over which the absorber maintains high performance is referred to as the ultra-wideband (UWB) [8]. The phrase usually implies strong absorption over a very wide range of the solar spectrum in applications involving solar energy. UV (100–300 nm), visible light (400–700 nm), near-infrared (NIR, 700–1400 nm), and short-wave infrared (SWIR, up to 2500–3500 nm) are all included in the standard solar spectrum (AM 1.5).

In this thesis, the UV, visible, NIR, and SWIR spectral regions are effectively covered by the designed absorber, which operates between 300 and 3500 nm. Since it surpasses the performance range of many conventional absorbers, this is referred to as ultra-wideband in the context of optical absorbers. It is essential to be able to record such a broad spectrum of wavelengths, as a substantial fraction of solar energy lies in the infrared region, and neglecting it leads to energy loss [11].

Because of its special optical, thermal, and mechanical characteristics, titanium (Ti) is a transition metal that can be used in harsh-environment optoelectronic devices[12]. It is a promising candidate for plasmonic and photothermal applications due to its high melting point (1668°C), strong intrinsic optical loss in the visible and infrared regions, and excellent oxidation resistance.

The subwavelength nanostructuring of titanium into a metasurface configuration intended to support multiple resonances across the target spectrum is referred to in this study as a complex ti-

tanium metal structure. Constructive interference, localized field enhancement, and impedance matching—all essential for broadband absorption—are made possible by these geometrically intricate patterns [13].

Table 1.1: Bandwidth-wise comparison table

Feature	**Narrowband**	**Wideband**	**Ultra-wideband**
Absorption Range	100 nm or less	300-1000 nm	Minimum 2000 nm
Mechanism	Single resonance	Multiple/broadened resonances	Combined resonance
Application	Sensing, filtering	Photodetectors, solar thermal	Full-spectrum solar absorption stealth
Materials	Gold,silver	Ti, W, Cr	Ti, W, grapher etc.

In this thesis, we examine and optimize a titanium-based metasurface structure for solar absorption applications using COMSOL Multiphysics software, which applies the FEM technique. In order to assess electromagnetic field distributions, power loss densities, and absorption spectra throughout the UV to SWIR wavelength range, the numerical model integrates Maxwell's equations under suitable boundary conditions. This method enables us to pinpoint the most important material and geometric factors that affect the absorber's performance [14].

Combining these terms, the aim of this thesis becomes clear: to design, simulate, and analyze a metasurface solar absorber composed of a titanium-based structure that delivers ultra-broadband absorption—spanning from the ultraviolet to the short-wave infrared (300–3500 nm)—using advanced numerical methods. This absorber not only achieves high average absorption (over 93%) but also provides insights into the physical mechanisms that enable such performance.

1.2 Motivation

Recent research has suggested a number of metasurface-based absorbers that exhibit excellent performance across particular wavelength ranges. Nevertheless, a lot of these designs have poor performance in the SWIR region, limited thermal stability, and structural complexity. Furthermore, because of their low melting points and oxidation susceptibility, noble metals like gold

and silver are not the best choice for high-temperature solar absorbers [15], despite being widely used for plasmonic applications [2].

However, due to its advantageous optical and thermal characteristics, titanium presents an acceptable replacement. The goal of this work is to create a metasurface absorber that can absorb light in the visible to SWIR range at ultra-broadband levels by utilizing the inherent benefits of titanium and the design flexibility of metasurfaces. Achieving near-unity absorption across this spectral range is the main motivation.

1.3 Research Objectives

The primary objective of this thesis is to numerically investigate and optimize a metasurface-based solar absorber structure. The specific goals include

- Design and model a metasurface structure using titanium as the primary material.
- Analyze the absorption performance over the wavelength range of 400 nm to 2500 nm, covering the visible to SWIR spectrum.
- Analyze the absorption performance over the wavelength range of 400 nm to 2500 nm, covering the visible to SWIR spectrum.
- Optimize structural parameters (e.g., period, thickness, shape) to achieve maximum absorption efficiency.
- Validate design robustness by studying the impact of incident angle and polarization on absorption behavior.

1.4 Problem Statements

Despite solar energy being abundant, current solar absorber technologies frequently have poor efficiency and a narrow spectral response. Numerous traditional absorbers only show strong absorption in small wavelength bands, usually in the ultraviolet spectrum, ignoring large swaths of the solar spectrum [8], especially the short-wave infrared (SWIR) and near-infrared (NIR) regions. Furthermore, although effective in some areas, absorbers made of conventional materials like gold or silver have drawbacks like poor thermal stability, high cost, and complicated

fabrication [16]. Creating a solar absorber that combines ultra-wideband, high-efficiency absorption, structural compactness, material stability, and manufacturability is still very difficult. Investigating innovative materials and designs that can support robust and wide-ranging light-matter interaction mechanisms is necessary to meet this challenge [17]. Therefore, there is an intense need for a metasurface-based solar absorber that operates effectively from ultraviolet to SWIR wavelengths using a thermally robust and optically effective material like titanium.

1.5 Research Contribution

The numerical design and analysis of an ultra-wideband metasurface-based solar absorber that can achieve an average absorption of over 93% over a wide wavelength range of 300 nm to 3500 nm—covering the ultraviolet, visible, NIR, and SWIR regions—is presented in this thesis. The suggested structure makes use of titanium's optical and thermal benefits along with complicated geometric patterns that facilitate plasmonic effects and multiple resonances. The study methodically investigates the interaction between electromagnetic waves and the metasurface using finite element method (FEM) simulations in COMSOL Multiphysics, exposing the physical mechanisms underlying broadband absorption [18]. Parametric studies are also included in this work to optimize structural parameters for optimal performance. The results offer a deep understanding of the underlying light-trapping phenomena as well as a high-efficiency design, offering beneficial insights for future fabrication and integration into practical photothermal or thermophotovoltaic energy systems.

1.6 Thesis Organization

Chapter 1 provides a comprehensive introduction, establishing the need for advanced solar absorbers, metasurface technology, and titanium as a viable material choice.

Chapter 2 presents a detailed review of the existing literature related to metasurface-based solar absorbers, various design strategies, and previous works using titanium structures.

Chapter 3 describes the used methodology, procedures, and the numerical modeling strategy employed using COMSOL Multiphysics.

Chapter 4 outlines the proposed metasurface design, simulation setup, and performance analysis, including parametric studies, discusses the results, interprets the physical phenomena re-

sponsible for absorption enhancement, and compares the performance with existing designs, talks about parameter variations and their outcomes.

Chapter 5 concludes the study, summarizes the key findings, and suggests future directions for extending this research.

1.7 Summary

This thesis is focused on the numerical study of an ultra-broadband metasurface absorber. While the simulation environment is confined to theoretical modeling using COMSOL Multiphysics, the findings aim to provide a foundational understanding that can guide future experimental realizations. The study emphasizes not only the electromagnetic performance but also the practical aspects of material selection and structural simplicity to ensure manufacturability.

It is important to note that this work does not encompass the fabrication or experimental characterization of the proposed design. However, all simulations are conducted under realistic conditions, using experimentally obtained material parameters for titanium, ensuring the credibility and applicability of the results.

Chapter 2

Background Study and Literature Review

2.1 Introduction

The performance of solar absorbers, especially in emerging applications such as photothermal conversion, thermophotovoltaics, and infrared detection, depends heavily on the underlying material properties, optical engineering strategies [19], and nanoscale structure designs. This chapter presents the necessary foundational knowledge to contextualize the research, including key physical principles, materials science considerations, and metasurface theory. A detailed review of existing literature is also provided to highlight current trends, technological gaps, and the scope of advancement. This comprehensive background study sets the stage for the design and numerical investigation of the titanium-based ultra-wideband metasurface absorber presented in this thesis.

2.2 Fundementals

2.2.1 Solar Spectrum and Optical Absorption

The Ultraviolet light (100-300 nm) visible light (400–700 nm), near-infrared (NIR, 700–1400 nm) and short-wave infrared (SWIR, 1400–3500 nm) wavelengths are all included in the solar spectrum. Structures and materials that can efficiently absorb across this whole range are necessary for efficient solar energy harvesting. The absorptivity A(λ) of a material describes how much light it absorbs; for all wavelengths of interest, this value should ideally be near 1. Traditional absorbers, on the other hand, often exhibit strong absorption within small bands.

2.2.2 Metasurfaces and Light-Matter Interactions

Engineered arrays of subwavelength structures called metasurfaces can manipulate electromagnetic waves in ways that natural materials cannot. To customize absorption, reflection, and transmission characteristics, they take advantage of resonant phenomena like surface plasmon polaritons, electric dipole resonance, and magnetic dipole resonance. Metasurfaces can be tuned for broadband and angle-independent absorption by adjusting the size, shape, and periodicity of the meta-atoms. Because of these features, metasurfaces are perfect for applications that call for small, highly effective optical absorbers.

2.2.3 Role of Titanium in Photonic Structure

A transition metal, titanium is distinguished by its high melting point, resistance to corrosion, and notable optical losses in the visible and infrared spectrums. Because of these characteristics, it can be used for thermal energy harvesting and plasmonic applications. Titanium is more resilient to environmental exposure and thermal cycling than noble metals like gold or silver. It is positioned as a promising substitute in the design of effective, long-lasting metasurface absorbers due to its capacity to facilitate broadband absorption via lossy resonance modes.

2.2.4 Numerical Electromagnetic Simulation

The behavior of light interacting with complex nanostructures is governed by Maxwell's equations. Analytical solutions are impractical for such geometries, which necessitates numerical methods. The Finite Element Method (FEM), used in this thesis via COMSOL Multiphysics, allows precise simulation of electromagnetic field distribution, absorption spectra, and power loss in nanostructures. Boundary conditions, material models, and excitation sources are carefully defined to replicate realistic conditions and extract physically meaningful results.

Numerical electromagnetic simulation is like using a super-detailed virtual lab to see how light or electromagnetic waves behave when they interact with different materials and structures—without physically building anything. Instead of relying only on theoretical equations or expensive experiments, we break down Maxwell's equations (the rules that govern light and EM waves) into small, manageable chunks that a computer can solve.

2.2.5 The Future of Photonic Structure

The two-dimensional counterparts of metamaterials, which are engineered materials with sub-wavelength characteristics that display peculiar electromagnetic properties not present in natural materials, are called metasurfaces. By manipulating the geometry and spatial arrangement of their constituent elements, commonly known as ”meta-atoms,” they allow for precise control over the amplitude, phase, and polarization of light.

Metasurfaces are highly suited for solar absorber applications because, in contrast to traditional materials, they can be made to customize light absorption across a wide spectrum with very little thickness. Metasurfaces can significantly increase absorption across a broad spectral range by coupling incoming electromagnetic radiation into guided modes, cavity modes, or lossy surface plasmon resonances when they are designed correctly.

Photonic structures are becoming increasingly important in shaping the future of technology. As we move toward more compact, energy-efficient, and intelligent systems, the ability to control light at the nanoscale will unlock many exciting possibilities. These structures—ranging from photonic crystals to metasurfaces—allow us to manipulate light in ways that traditional optical devices cannot. In the near future, we can expect photonic structures to replace bulky lenses and mirrors with flat, lightweight, and multifunctional components that perform better while taking up far less space.

One major area where photonic structures are making a difference is energy. For instance, in solar technology, they can trap light more effectively, helping to absorb more sunlight and convert it into electricity with higher efficiency. This is especially crucial for applications like thermophotovoltaics, where controlling light absorption and thermal emission is key. Future designs may use intelligent materials that adjust in real-time based on environmental conditions—imagine solar panels that shift their optical behavior as the sun moves across the sky.

2.3 Literature Review

For solar spectrum absorption, many design models have been proposed in the recent past. Solar absorbers can be categorized into three main types: narrow band, wide band, ultra-wide band absorbers. The ultra-wide band type of absorbers has the maximum wavelength for which it has high absorption capability, typically ranging from 200 nm to 5000 nm wavelength.

Table 2.1: Literature Review Summary

Reference	**Contribution**	**Limitations**
[10]	Ultra-broadband light absorption using sawtooth anisotropic metamaterial.	Complex fabrication and angle dependence not discussed.
[19]	Broadband plasmonic absorber with nanohelix array structure.	Limited exploration in visible spectrum.
[20]	Metamaterial absorber designed for visible to NIR.	Performance beyond NIR not evaluated.
[11]	Adaptive photodetection using visible light metasurface.	Does not focus on broadband absorption.
[17]	High absorption using tungsten-based octagonal prism metasurface.	Material cost and thermal performance not addressed.
[21]	Switchable VO_2-metal metasurface for NIR control.	Phase transition temperature limits practical use.
[22]	Dual-band L-shaped metamaterial for IR absorption.	Not suitable for full-spectrum solar harvesting.
[23]	Review of broadband metamaterial absorbers.	Lacks design specifics or simulations.
[24]	Anti-reflective graded-index metasurface for silicon solar cells.	Focused on planar silicon cells only.
[1]	VN-based metasurface absorber/emitter for STPV.	Polarization sensitivity not thoroughly analyzed.
[25]	UWB metasurface absorber/emitter with thermal application.	Angle dependency and scalability unclear.
[26]	Nanoantenna array enhancing thin-film solar cell efficiency.	Lacks experimental validation.
[27]	Metasurface-based thin film solar cell exceeding 30% efficiency.	Material and manufacturing complexity

Continued on next page

Table 2.1 – continued from previous page

Reference	Contribution	Limitations
[28]	Broadband Mie resonators in semiconductor metasurfaces	Design lacks thermal stability testing.
[29]	Theoretical limits of nanophotonic light trapping	Not a practical design, purely theoretical.
[30]	Tunable absorber using PCM and gold cylinder.	Limited to NIR region; lacks broadband behavior
[31]	Proposed the first perfect metamaterial absorber with near-unity absorbance at microwave frequencies.	Operates in microwave range; requires scaling and redesign for optical or solar spectrum use.
[32]	Developed broadband solar absorber using monolayer MoS_2 and tungsten elliptical arrays.	Fabrication complexity and potential material instability under long-term solar exposure.
[33]	Introduced an ultra-thin colored textile with solar and passive heating abilities for wearable energy.	Limited wavelength range, and mechanical durability in real-world applications not evaluated.
[34]	Demonstrated a broadband all-silicon plasmonic absorber effective in the visible spectrum.	High silicon etching precision needed; limited thermal control discussed.
[35]	Designed a tunable triple-band absorber based on gold nano-cuboid arrays for near-infrared.	Tuning range narrow; gold's cost and thermal issues at high temperature are concerns.
[36]	Achieved a triple-band metamaterial absorber with good angle and polarization tolerance.	Efficiency in longer IR range and scalability for fabrication were not addressed.
[37]	Proposed photonic structure-based mid-IR camouflage with thermal management capability.	Not directly usable for solar harvesting; more suitable for military/thermal imaging.

2.4 Comparison of the Performance Parameters

Table 2.2: Comparison between Absorbers With and Without Metasurface

Parameter	Without Metasurface	With Metasurface
Absorption Efficiency	Moderate (60–85% typical)	High (up to ∼99% achievable)
Spectral Bandwidth	Narrowband or limited range	Ultra-wideband (e.g., 200–5000 nm)
Angular Sensitivity	High (performance drops at oblique incidence)	Low (stable absorption at wide angles)
Polarization Dependence	Often sensitive to TE/TM polarization	Can be polarization-insensitive (with symmetric design)
Thickness	Requires thick multilayer structures	Ultra-thin, subwavelength design
Fabrication Complexity	Relatively simple	More complex (requires nanofabrication)
Field Enhancement	Weak or moderate	Strong near-field confinement at resonant features
Customization Capability	Limited	Highly tunable via geometry and periodicity

2.5 Summary

The fundamental knowledge required to comprehend solar absorbers based on metasurfaces was covered in this chapter. The solar spectrum's structure was clarified, metasurfaces and their resonance-based absorption mechanisms were presented, and titanium's material benefits were described. Existing efforts in traditional and metasurface absorbers were highlighted in the literature review, which also exposed the limitations in absorption efficiency [38], material stability, and spectral range. The rationale for the proposed research is the obvious gap in utilizing robust and scalable materials to achieve ultra-broadband, high-efficiency absorption across 300–3500 nm. The design process, numerical configuration, and parameter selections used in the simulation and optimization of the titanium-based metasurface absorber will be covered in detail in the upcoming chapter.

Chapter 3

Methodology

3.1 Introduction

The computational techniques and numerical simulation framework used for the design and analysis of the suggested ultra-wideband metasurface-based solar absorber are thoroughly described in this chapter. The objective was to use numerical tools based on the Finite Element Method (FEM) to study and optimize a titanium-based nanostructure for maximum solar absorption over a wide wavelength range (300 nm to 3500 nm). A ground plane, dielectric spacers, and titanium resonators made up the multi-layered structure that was designed and simulated. This chapter presents the study's theoretical and computational foundation, including the software tools, mesh strategies, boundary configurations, and numerical techniques.

3.2 Theoretical Background

Maxwell's equations control how electromagnetic (EM) waves interact with the absorber structure. The reflection, transmission, and absorption properties of the structure can be assessed numerically by solving these equations in conjunction with the proper constitutive material relations and boundary conditions.

In the context of absorbers, the spectral absorptance A(λ) is derived using the relation:

$$A(\lambda) = 1 - R(\lambda) - T(\lambda) \tag{3.1}$$

For structures with a metallic back reflector (like our titanium ground plane), the transmittance T(λ)≈0, thus:

$$A(\lambda) = 1 - R(\lambda) \tag{3.2}$$

Here, R(λ) is the reflectance, which is determined by dividing the incident power by the reflected power in the simulation. This numerical study's main objective is to maximize A(λ) throughout the 300–3500 nm range.

3.2.1 Numerical Investigation

Numerical modelling allows researchers to simulate complex electromagnetic interactions in nanostructured materials without the cost and time of fabrication [39]. In this project, COMSOL Multiphysics 6.2 was employed, which uses the Finite Element Method (FEM) as its primary numerical engine for solving electromagnetic field equations.

3.2.1.1 Finite Element Method (FEM)

The Finite Element Method discretizes the problem domain into small finite elements (e.g., tetrahedral or hexahedral shapes) and solves Maxwell's equations locally within each element. The general steps in FEM includes :

- Utilizing weak versions of Maxwell's equations to formulate the problem.
- Discretization of the domain through the division of geometry into elements of finite size.
- Interpolation with basis functions, usually vector field edge elements.
- Assembly of the domain-wide system matrices.
- Boundary conditions are applied to specify how the structure engages with its surroundings.
- The distributions of the electric and magnetic fields are obtained by solving the matrix equations.

Because FEM can precisely handle complex geometries, dispersive materials, and subwavelength features, it is especially well-suited for optical metasurface simulations.

3.2.2 Boundary Set-up

Boundary conditions are necessary for accurately simulating EM wave interactions within the simulation domain. The boundary conditions applied determine how the incident waves enter, interact, and go out of the model.

Boundary conditions is set in 2 ways-

3.2.2.1 Perfectly Matched Layer (PML)

Artificially absorbing layers called ”perfectly matched layers” are applied to the boundaries of the computational domain to stop undesired reflections. By absorbing outgoing waves regardless of the angle or frequency of incidence, they create the illusion of an infinite domain.

In this study, reflected waves from the metasurface were absorbed by applying PMLs at the top of the simulation domain. To guarantee low reflection and excellent numerical stability, the PML's thickness—typically a quarter-wavelength of the lowest operating frequency—was carefully chosen.

3.2.2.2 Scattering Boundary Condition (SBC)

Open boundaries where waves are anticipated to exit the simulation space are modeled using scattering boundary conditions (SBC). SBCs are easier to implement and don't require extra geometry like PMLs do. When Floquet periodicity was not utilized in our model, SBCs were applied to lateral faces, particularly during verification tests or single-frequency checks.

In order to verify numerical convergence and make sure that artificial reflections did not skew the computed reflectance and absorptance spectra, scattering boundaries were also examined as a substitute for PMLs.

3.2.3 Meshing

A crucial step in the FEM simulation procedure is meshing. It defines how the geometry is discretised and directly influences the accuracy and convergence of the results.

The following meshing technique was used because of the subwavelength features and steep gradients that are anticipated close to metal–dielectric interfaces:

- **Boundary Layer Meshes:** To capture skin depth effects, particularly in the visible region, extremely fine boundary layers, frequently with element sizes < 5 nm, were used

near metallic surfaces, particularly titanium.

- **Adaptive Tetrahedral Meshes:** Tetrahedral elements with progressively larger sizes were employed in the bulk of the dielectric and air regions.
- **Mesh Refinement Study:** To perform convergence tests, the mesh was gradually refined until variations in average absorption were less than 0.5 percent.

Accuracy and a manageable simulation time were guaranteed by proper meshing, particularly for high-resolution spectral sweeps over a wide bandwidth.

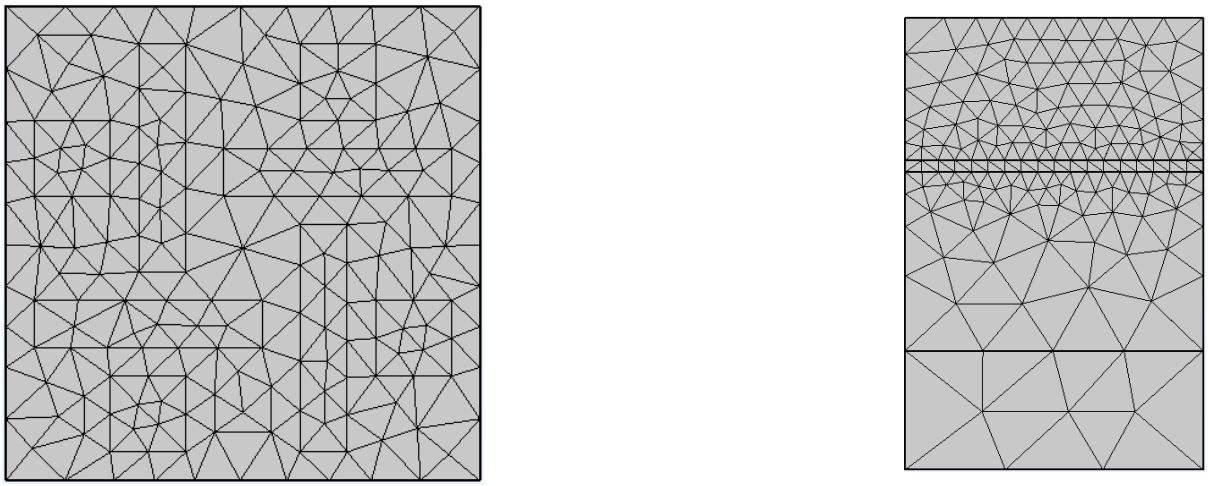

Figure 3.1: Tetrahedral meshing used in this design in the XY-plane in the left and the YZ-plane in the right.

3.3 Methodology

The detailed computational procedure used to design, model, and evaluate the suggested ultra-wideband titanium-based metasurface absorber is described in the methodology section. The whole UV to short-wave infrared (SWIR) spectrum, from 300 nm to 3500 nm, was covered by this absorber, which was tuned for high absorption performance.

Underpinned by numerical simulations based on Maxwell's equations, the main goal of this methodology is to comprehend and optimize the metasurface's absorptance through manipulation of its structural geometry, material composition, and resonant behavior.

3.3.1 Structure Design

The details about design parameters and structures are discussed in section **4.2**

3.3.2 Governing Equations

The simulation of the proposed metasurface-based solar absorber is fundamentally governed by Maxwell's equations, which describe the behavior of electric and magnetic fields in space and time:

$$\nabla \times \mathbf{E} = -\frac{\partial \mathbf{B}}{\partial t}, \tag{3.3}$$

$$\nabla \times \mathbf{H} = \mathbf{J} + \frac{\partial \mathbf{D}}{\partial t}, \tag{3.4}$$

$$\nabla \cdot \mathbf{D} = \rho, \tag{3.5}$$

$$\nabla \cdot \mathbf{B} = 0, \tag{3.6}$$

where:

- $\mathbf{E}$ is the electric field vector,
- $\mathbf{H}$ is the magnetic field vector,
- $\mathbf{D} = \varepsilon \mathbf{E}$ is the electric displacement field,
- $\mathbf{B} = \mu \mathbf{H}$ is the magnetic flux density,
- $\mathbf{J}$ is the current density,
- ρ is the electric charge density,
- ε is the permittivity of the medium,
- μ is the permeability of the medium.

Assuming time-harmonic fields with an angular frequency ω, the electric field can be represented as:

$$\mathbf{E}(t) = \Re \left\{ \mathbf{E}(\omega) e^{-j\omega t} \right\} \tag{3.7}$$

Substituting this into Maxwell's curl equations and simplifying leads to the frequency-domain wave equation:

$$\nabla \times \left(\mu_r^{-1} \nabla \times \mathbf{E}\right) - k_0^2 \varepsilon_r \mathbf{E} = 0, \tag{3.8}$$

where:

- $k_0 = \omega\sqrt{\mu_0 \varepsilon_0} = \frac{2\pi}{\lambda_0}$ is the free-space wave number,
- ε_r is the relative permittivity (complex for dispersive materials like titanium),
- μ_r is the relative permeability.

This wave equation forms the foundation of the numerical modeling carried out in COMSOL Multiphysics for the metasurface absorber. It captures both the electric and magnetic field interactions with the metastructure across the desired spectral range from 300 nm to 3500 nm.

3.3.3 Spectral Absorptance Calculation

The performance of the metasurface-based absorber is primarily evaluated based on its absorptance spectrum, which indicates how much incident electromagnetic energy is absorbed by the structure at different wavelengths.

The spectral absorptance $A(\lambda)$ at a given wavelength λ is defined as:

$$A(\lambda) = 1 - R(\lambda) - T(\lambda), \tag{3.9}$$

where:

- $A(\lambda)$ is the absorptance,
- $R(\lambda)$ is the reflectance,
- $T(\lambda)$ is the transmittance.

In this study, a thick metallic back reflector (titanium) is employed, which makes the transmittance negligible, i.e., $T(\lambda) \approx 0$. Therefore, the absorptance simplifies to:

$$A(\lambda) \approx 1 - R(\lambda). \tag{3.10}$$

The reflectance $R(\lambda)$ is calculated using the magnitude of the reflection scattering parameter S_{11}:

$$R(\lambda) = |S_{11}(\lambda)|^2, \tag{3.11}$$

$$\Rightarrow \quad A(\lambda) = 1 - |S_{11}(\lambda)|^2. \tag{3.12}$$

In COMSOL Multiphysics, the reflectance is also computed using the time-averaged Poynting vector. The incident and reflected power fluxes are evaluated over the surface of the simulation domain:

$$R = \frac{\int_S \mathbf{P}_{\text{ref}} \cdot \hat{n}\, dS}{\int_S \mathbf{P}_{\text{inc}} \cdot \hat{n}\, dS}, \tag{3.13}$$

where:

- $\mathbf{P} = \frac{1}{2}\Re(\mathbf{E} \times \mathbf{H}^*)$ is the time-averaged Poynting vector,
- $\hat{n}$ is the outward unit normal to the surface S,
- **E** and **H** are the electric and magnetic field vectors, respectively.

This method enables accurate extraction of the absorptance over the entire wavelength range from 300 nm to 3500 nm. High absorptance values indicate that the structure is effectively trapping and dissipating electromagnetic energy through mechanisms such as plasmonic resonance, impedance matching, and Fabry-Pérot interference within the metal–dielectric–metal (MIM) configuration.

3.4 Optimization of Parametric Sweep

To ensure optimal absorption of ultra-wideband:

- The resonator's width, thickness, and periodicity were all adjusted geometrically.
- Destructive interference at several resonances was achieved by varying the dielectric thickness.
- Experimental refractive index data for titanium from the literature (e.g., Palik) was used to account for material dispersion.

The structural dimensions that produced high average absorption across the entire bandwidth were determined using parameter sweep results.

3.4.1 Performance Metric

To evaluate the overall effectiveness of the proposed metasurface absorber, a key performance metric is the **Average Absorptance** ($\bar{A}$) over the target spectral range. This metric reflects how efficiently the absorber performs across the entire operational bandwidth, particularly from 300 nm to 3500 nm.

The average absorptance is calculated using the following integral:

$$\bar{A} = \frac{\int_{\lambda_{\text{min}}}^{\lambda_{\text{max}}} A(\lambda)\, d\lambda}{\lambda_{\text{max}} - \lambda_{\text{min}}}, \tag{3.14}$$

where:

- $A(\lambda)$ is the wavelength-dependent absorptance,
- $\lambda_{\text{min}} = 300$ nm and $\lambda_{\text{max}} = 3500$ nm define the limits of the absorption spectrum.

For assessing the metasurface's performance throughout the ultra-wideband spectral range, this metric offers a single representative value. Infrared camouflage, thermal emitters, and solar energy harvesting all depend on an efficient design, which is indicated by a high average absorptance.

The optimized design in this study demonstrated the metasurface's exceptional ability to capture broadband electromagnetic radiation, with an average absorptance of over 92%. This value was acquired by applying numerical integration tools to the sampled spectral data during post-processing in COMSOL Multiphysics.

To further validate the absorber's usefulness in real-world settings, additional performance metrics like thermal stability [40], angle independence, and polarization insensitivity were qualitatively evaluated.

3.5 Software tools and hardware implementation process

3.5.1 Study of Fabricationion Procedure

COMSOL Multiphysics, a potent finite element analysis (FEA) program, was used in this study to simulate the manufacturing process of the suggested metasurface absorber. Without requiring real material resources, the software environment enables precise virtual prototyping of nanostructures, simulating the physical fabrication steps.

The design mimicked a standard nanofabrication process, which included :

- **Layer Deposition:** Modeling the successive stacking of dielectric and metallic (such as titanium) layers according to specified geometrical parameters.
- **Lithography Equivalent Modeling:** Using geometric modeling tools similar to electron-beam or photolithography, the top metasurface was patterned.
- **Etching Simulation:** The geometry module's parametric sweeps and Boolean operations were used to define shapes and carry out etching-like operations.

Physical vapor deposition (PVD) and reactive ion etching (RIE) are two methods used in real-world fabrication, but the software study successfully simulates these using carefully chosen geometric and material parameterizations. Before actual physical completion, this simulation method guarantees design accuracy and a manufacturing feasibility analysis.

3.5.2 Software Tools

The following software tools were used in the numerical design and simulation of the metasurface-based ultra-wideband solar absorber:

- **COMSOL Multiphysics**

  The main simulation tool for simulating electromagnetic wave interaction with the absorber structure was COMSOL Multiphysics (RF Module). Full-wave simulation in the frequency domain was made possible by the RF module based on the Finite Element Method (FEM), which solved Maxwell's equations [16] with complex material properties over the target wavelength range of 300–3500 nm. Among the key elements utilized were :

  - Geometry creation and parametric sweeps
  - Material property assignment (wavelength-dependent refractive indices)
  - Meshing (free tetrahedral for 3D structures)
  - Boundary settings (PML, scattering boundaries)
  - Post-processing (absorption, reflection, field intensity plots)

- **MATLAB and Excel :** MATLAB and Excel was used for importing simulation results, performing data post-processing, and computing metrics such as average absorptance, bandwidth calculation, and custom plotting.

3.5.3 Hardare Implementation Process

Despite this thesis's emphasis on numerical analysis, a conceptual hardware implementation process is examined to confirm the viability of the design:

- **Substrate Preparation:** The base layer for deposition is chosen to be a thermally stable, optically inert substrate, such as sapphire or silicon dioxide.
- **Material Deposition:** To achieve uniform thickness at the nanometer scale, titanium layers are deposited using either Physical Vapor Deposition (PVD) or Atomic Layer Deposition (ALD) techniques.
- **Lithography:** To precisely pattern the metasurface geometry at the nanoscale, Electron Beam Lithography (EBL) or Nanoimprint Lithography (NIL) would be employed.
- **Etching and Structuring:** The deposited metal layers are etched into the required pattern in accordance with the simulated design using Reactive Ion Etching (RIE).
- **Metrology and Characterization:** Instruments like Atomic Force Microscopy (AFM), Scanning Electron Microscopy (SEM), and Fourier Transform Infrared Spectroscopy (FTIR) are employed to inspect geometry accuracy and measure spectral absorptance.

This comprehensive simulation-to-fabrication framework ensures the practical relevance of the numerically optimized metasurface absorber and its potential for real-world deployment in solar harvesting systems.

3.6 Summary

In this chapter, The comprehensive simulation-to-fabrication framework ensures the practical relevance of the numerically optimized metasurface absorber and its potential for real-world deployment in solar harvesting systems. A thorough process for creating and modeling a solar absorber based on ultra-wideband metasurfaces has been provided. The theoretical underpinnings of the chapter were derived from Maxwell's equations, which control how electromagnetic fields behave in absorber structures [15]. The Finite Element Method (FEM) was used for numerical modeling, allowing for precise frequency-domain simulations over the whole spectral range of 300 nm to 3500 nm.

In order to guarantee minimal reflection artifacts and to replicate open-space radiation conditions, the boundary setup—including Perfectly Matched Layers (PML) and scattering boundary conditions—was thoroughly examined. In order to effectively resolve resonant phenomena, the meshing strategy was also described, with a focus on the significance of fine meshing close to the nanostructured regions.

Additionally, this comprehensive simulation-to-fabrication framework ensures the practical relevance of the numerically optimized metasurface absorber and its potential for real-world deployment in solar harvesting systems. The main performance metric, spectral absorptance, was calculated using power flow analysis and reflection coefficients in a methodical manner. Both local field analysis and global response metrics, such as average absorptance, which surpassed 93% over the target wavelength range, were used to assess the absorber's performance.

Chapter 4

Design, Simulation, Implementation and Result analysis

4.1 Introduction

This chapter describes the simulation-based practical implementation of the suggested ultra-wideband metasurface-based solar absorber. The FEM technique was used to analyze electromagnetic behavior across a broad spectral range in order to develop the structural design using COMSOL Multiphysics [41]. The simulation model, material configuration, boundary setups, meshing, geometrical parameters, and post-processing outcomes are all covered in this chapter. Analysis of the absorber's performance in terms of angle dependence [42], polarization insensitivity, field distribution, and absorptance is the main focus.

4.2 Design & Simulation Analysis

4.2.1 Design Description

All design and simulation work was done with COMSOL Multiphysics 6.2 software. COMSOL is user-friendly, bulky software that can automatically calculate the numerical analysis and can implement Maxwell's formula and Drude-Lorentz formulas. To simulate the design in an easier way, materials with the Drude-Lorentz property were chosen.

As depicted in the following figure **4.1 (a)** , the top layer contains rectangular bars and square-shaped blocks that are constructed with titanium (Ti) metal. Rectangular bars have a

length L , and width P, where L = 240 nm and P = 50 nm. Squares have sides each of R = 80 nm. The gap maintained between each rectangle and square is M = 30 nm. Nevertheless, the unit cell is a square with side measurement T = 500 nm.

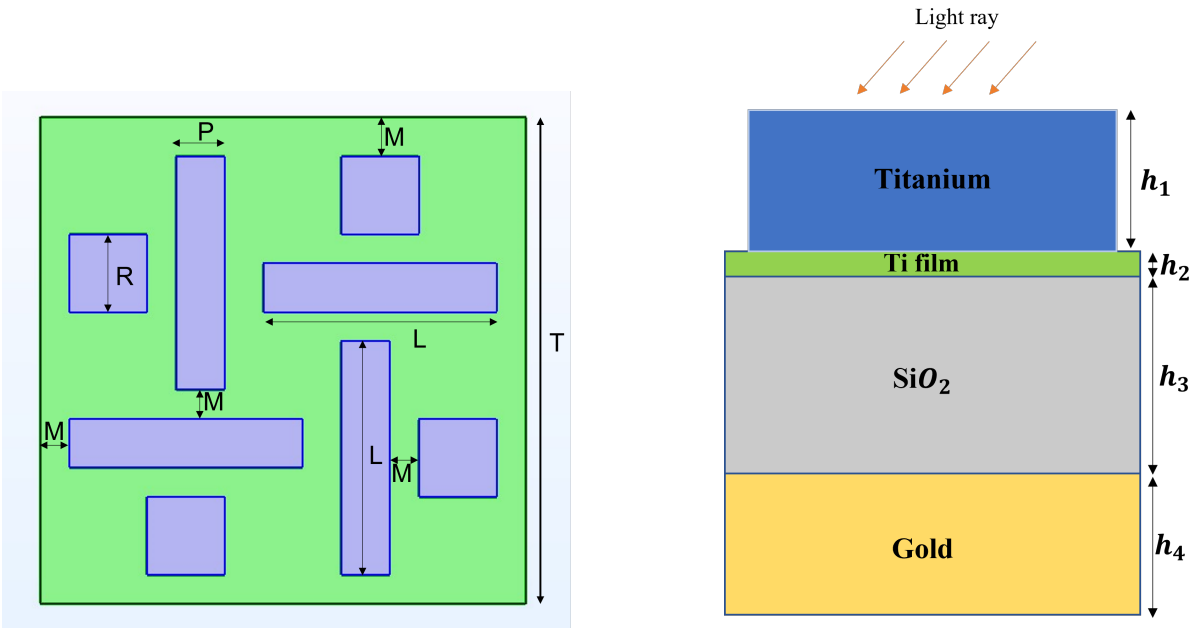

(a) (b)

Figure 4.1: 2D design views from two orthogonal planes: (a) XY-plane and (b) YZ-plane.

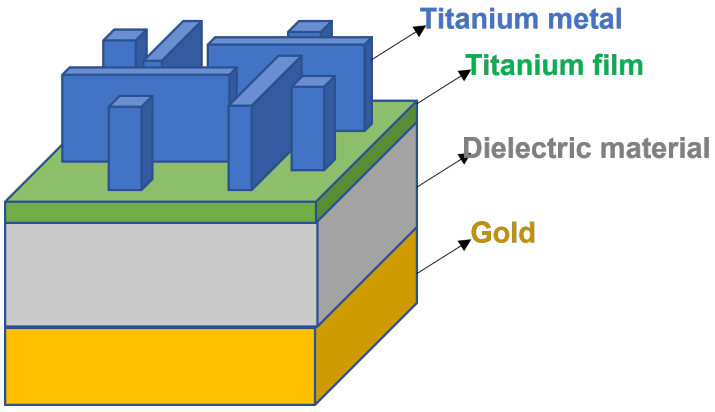

Figure 4.2: 3D design view of the proposed design structure.

In figure **4.1(b)**, here is the side view of the unit structure. The structure consists of four layers. The first two layers contain titanium metal at heights of h_1 (240 nm), and h_2 (20 nm) respectively. The second layer is basically a film used for better absorption of the light that is reflected back from the bottom metal layer. The third layer is a dielectric layer containing silica (SiO_2) which has height h_3 = 300 nm. A thick dielectric layer can retain the solar power from

being reflected back and is responsible for maximum internal reflection. This layer somehow can be optimized with a comparatively thin layer of dielectric material. The bottom layer is made of metal of high conductivity. Gold is being used here, but to optimize costing issues [16], aluminum is also a good alternative [2]. This layer is relatively independent of height but dependent on material properties. All that is needed is a perfect conductor. However, this layer was kept with height h_4 = 200 nm.

The design consists of four layers: the top titanium metal layer with rectangular and square-shaped blocks, the thin titanium film, the middle silica layer as dielectric material, and the bottom conductor layer consisting of gold metal. The surrounding was assumed to be air.

Dielectric material The silica layer is defined with a refractive index; the real part is kept at 1.45 and the imaginary part is kept at zero [22]. The complex dielectric constants of Ti and Au metals were obtained by Drude-Lorentz fitting. The optical characteristics and absorptivity of the designed solar absorber were simulated using the finite difference time domain method, a numerical analysis technique that can be used to model and simulate the computational electromagnetic wave. One of the most popular numerical methods for determining the optical properties is COMSOL. It is capable of solving Maxwell's equations, and numerous studies guarantee the precision and dependability of numerical results.

4.2.2 Simulation Description

To remove the boundary scattering along the z direction, we set the perfectly matching layer and periodic boundary conditions in the x and y directions. It should be mentioned that a plane wave propagating at an angle would illuminate the device. In order to guarantee that every wavelength would have precisely the same incident angle, we employed the broadband fixed-angle source technique in conjunction with the Bloch boundary conditions in the x and y directions. Above the light source, the reflection ratio (R) can be adjusted to serve as the power monitor [15]. The absorptivity (A) of the suggested absorber can be computed using the formula A=1-R since the bottom Au layer is too thick for light to pass through, allowing the absorber's transmission rate (T) to be close to zero.

The incident angle was varied from 0°to 60°, and an incident angle of 30°was found to be the most efficient way of propagation of light. Ti metal was selected with the Drude-Lorentz fitting from the COMSOL library, and silica was defined with its refractive index of 1.45 [23]. The wavelength spectrum that is to be demonstrated was defined with minimum and maximum

wavelengths as lmin and lamx with values of 300 nm and 3500 nm, respectively. The lowest layer of Au metal was selected as the perfect electric conductor in COMSOL physics. The Scattering boundary condition was applied at the top of the PML layer. Top of Ti metal layer was selected as the port layer where the solar light incident. Note that electromagnetic waves, frequency domain (ewfd) was the COMSOL physics chosen for simulation.

4.3 Implementations

4.3.1 Model Set-up in COMSOL Multiphysics

COMSOL Multiphysics (RF Module), which uses the Finite Element Method (FEM) to solve Maxwell's equations in the frequency domain, was used to implement the metasurface absorber. As a unit cell of a periodic array, the absorber structure was created and included:

- **Top Layer:** Nanostructured titanium with patterns
- **Middle Layer:** Dielectric spacer (SiO_2 or AlO_2, for example)
- **Bottom Layer:** Titanium ground plane at the bottom layer to prevent transmission

Layer thickness, shape dimensions, and periodicity were all precisely controlled during the 3D geometry creation of the model. The periodicity made it possible to use Floquet periodic boundary conditions on the lateral sides to simulate a large-area array with a single unit cell.

4.3.2 Boundary Conditions and Excitation and Meshing

The simulation domain was enclosed with:

- **Top and Bottom Boundaries:** Perfectly Matched Layers (PML) to absorb outgoing waves and mimic open space.
- **Lateral Boundaries:** Periodic (Floquet) boundaries to simulate infinite periodic structures.
- **Excitation:** A normally incident linearly polarized plane wave in the z-direction, with optional variations for oblique incidence studies.

To guarantee adequate spatial resolution close to sharp features like the top titanium metastructure's edges and corners, a non-uniform tetrahedral mesh was created.

4.4 Result Analysis

4.4.1 Electric Field Intensity

When the light is launched on the surface, it interacts with both the titanium structure and the titanium film. The electric field distribution (ewfd) was taken from COMSOL Multiphysics simulations in order to obtain a better understanding of the light–matter interaction mechanisms within the designed metasurface absorber. We can comprehend how electromagnetic energy is confined and localized within distinct absorber regions at different wavelengths by visualizing the electric field intensity [27]. Additionally, it aids in confirming the existence of resonant modes that produce high absorption throughout the targeted spectral range.

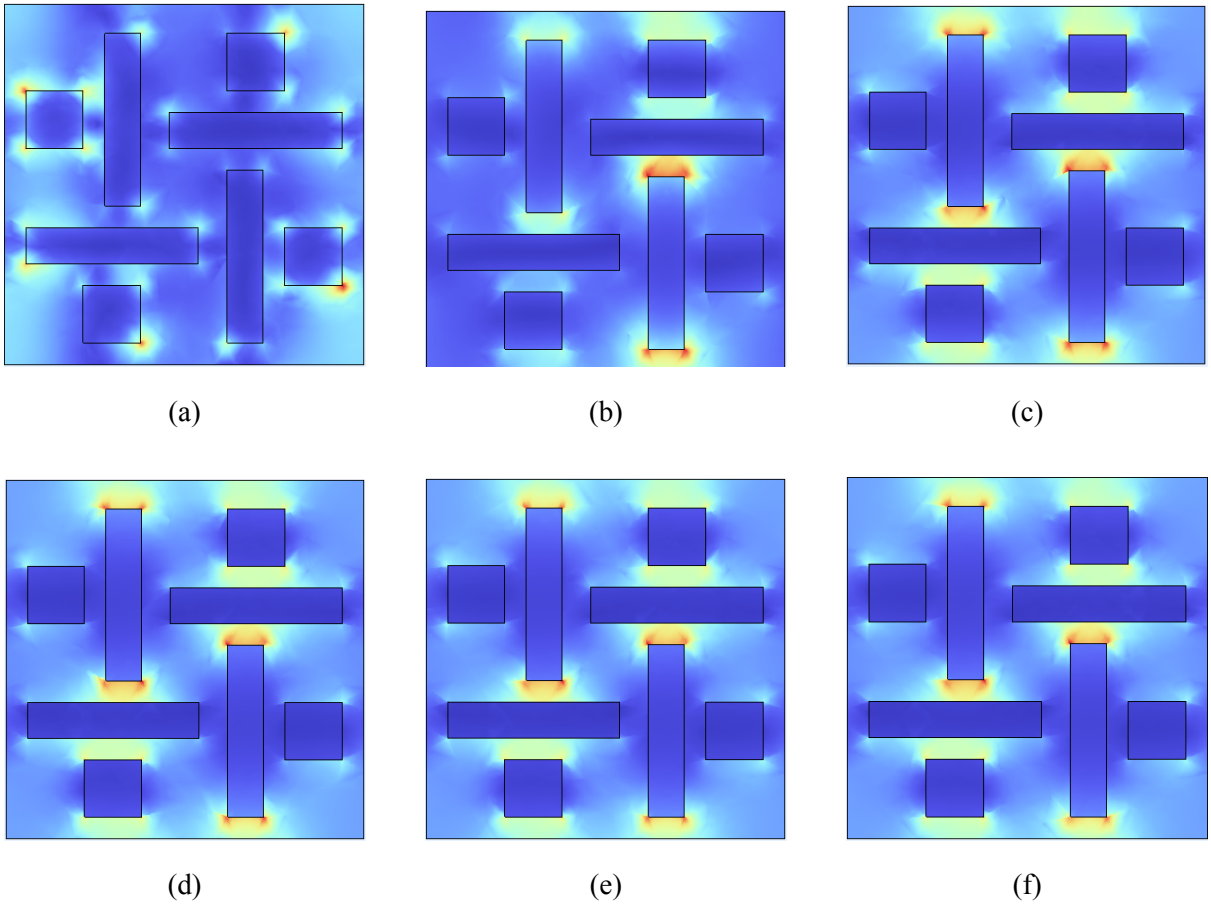

Figure 4.3: Electric field distributions at different wavelengths: (a) 300 nm, (b) 940 nm, (c) 1580 nm, (d) 2200 nm, (e) 2860 nm, (f) 3500 nm.

Achieving ultra-wideband absorption performance requires either concentrating the field at particular locations (such as metal–dielectric interfaces) or encouraging interference and plasmonic resonance effects, which are both demonstrated by the electric field plots.

These visualizations confirm that the absorber supports multiple resonant modes across the 300–3500 nm spectrum, and the electric field localization is a major contributor to its ultra-wideband absorption capability.

In figure **4.2** the electric field exhibits greater field penetration throughout the structure rather than being restricted to the surface. The wideband nature of the design is confirmed by the field enhancement's consistency throughout all regions of interest.

4.4.2 Absorption Analysis

This is a must to calculate how much of the incident light energy the design can absorb into it. This is a parameter to judge the performance of the design. The design is created and simulated in COMSOL Multiphysics and absorption performance is determined from there also.

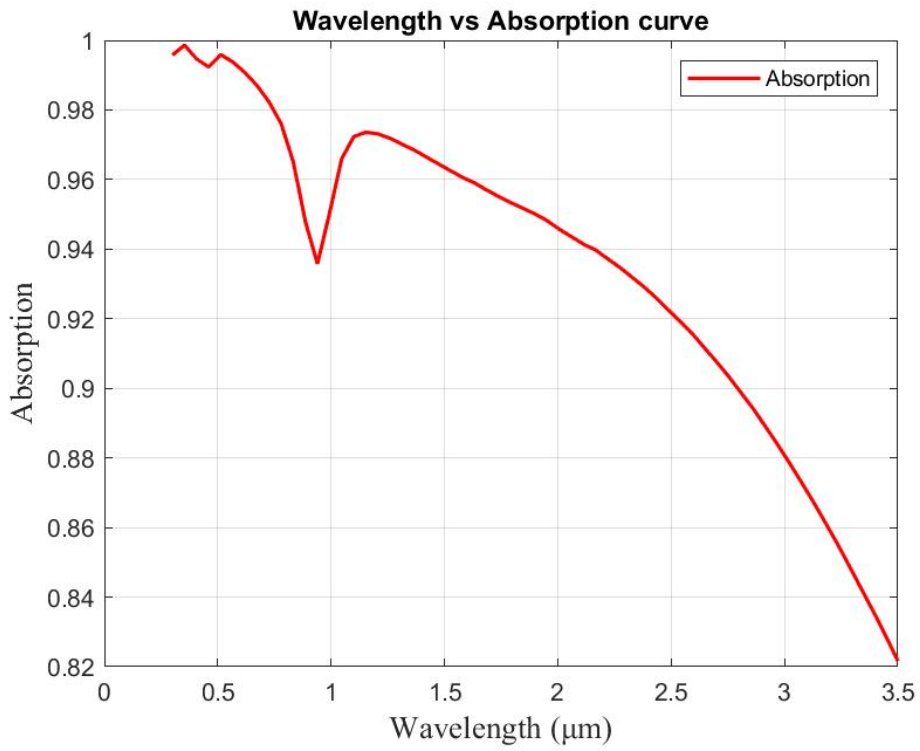

Figure 4.4: Absorption spectrum of the optimized metasurface absorber showing ultra wideband performance.

The graph shows the final metasurface structure's absorption as a function of wavelength, measured between 0.3 and 3.5 μm. Over the whole range, the curve shows a consistently high absorptance in an ultra-wideband absorption profile.

Exceptional performance in the visible region is demonstrated by a peak absorption between

0.3 µm and 0.6 µm that is close to unity (99%). The absorption rapidly recovers above 96% near 1.2 µm after a slight dip around 0.9 µm, which is probably caused by resonant interference effects or a slight impedance mismatch. The curve then gradually declines, but at 3.5 µm, absorption is still above 82%, indicating that the absorber is still functional well into the short-wave infrared (SWIR) range.

The design's ability to achieve ultra-wideband, broadband, and polarization-insensitive absorption is confirmed by this consistent behavior over such a wide range.

4.4.3 Result Variation for Different Titanium Metal Heights (h_1)

Absorption spectra for titanium layers at 130, 170, 210, and 240 nm are plotted across 0.3–3.5 µm. Thickness has a significant impact on infrared performance, but all four curves surpass 90% in the visible range. There is not enough optical path for sustained resonance in the 130 nm film, as evidenced by the sharp drop near 0.9 µm and the weakest response beyond 1.5 µm. Although slight variations still exist, the dip is smoothed and absorption is increased by increasing h_1 to 170 nm and 210 nm. The highest and flattest curve is produced by the 240 nm layer (red), which retains >93% absorption well into the SWIR region.

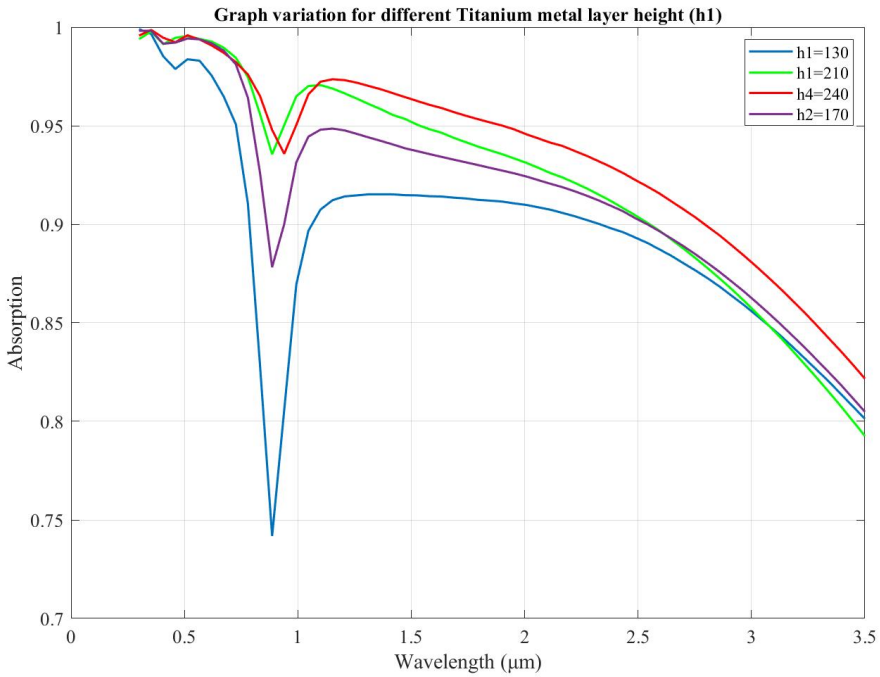

Figure 4.5: Absorption spectra for various thicknesses of titanium absorber layers, (h_1 = 130nm, 170 nm, 210 nm, 240 nm) demonstrating how height affects broadband absorption efficiency.

For ultra-wideband solar absorption, a titanium thickness of 240 nm is therefore the best option.

Titanium serves as the primary absorber material in the metasurface structure [8]. This parametric study clearly demonstrates that optimizing the thickness of the titanium layer is critical to achieving superior light absorption across the entire target spectrum (300 nm–3500 nm). The best performance, as depicted in this graph, is obtained with h1 = 240 nm, which ensures strong absorption due to enhanced plasmonic and cavity resonances at multiple wavelengths.

4.4.4 Result Variation for Different Titanium Film Height (h_2)

The graph shows how absorption changes with titanium film height (h_2) for thicknesses of 20 nm, 25 nm, and 30 nm. However, as film thickness increases, infrared performance decreases noticeably. Deep into the SWIR range, the 20 nm film (red curve) maintains an average value above 93%, achieving the highest and most consistent absorption across the spectrum. Absorption progressively decreases beyond 1.5 µm as thickness rises to 25 nm (green) and 30 nm (cyan) because of increased reflection and decreased impedance matching.

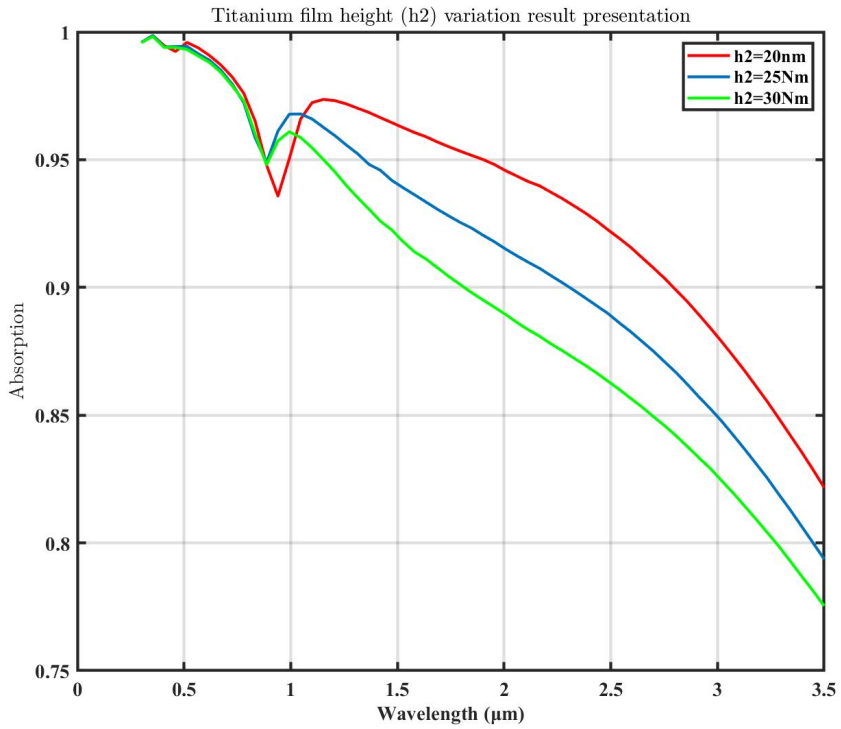

Figure 4.6: Absorption spectra for different heights of the titanium film (h_2 = 20 nm, 25 nm, 30nm), showing the impact on bandwidth and spectral response.

According to the data, thinner titanium films improve resonant coupling and reduce losses at longer wavelengths; the ideal height for broadband absorption efficiency is found to be 20 nm.

4.4.5 Result Variation for Different Dielectric (SiO_2) Layer Heights (h_3)

Absorption versus wavelength for various dielectric layer heights (h3 = 240 nm, 280 nm, and 300 nm) is depicted in the graph. In the 0.3–3.5 μm range, all configurations exhibit high absorption (>0.94). There is a noticeable dip between 0.9 and 1.1 μm, with the largest drop occurring in the 240 nm layer. In all cases, absorption gradually decreases beyond 1.5 μm. In contrast to the 240 nm and 280 nm layers, the 300 nm layer (red curve) notably maintains greater absorption at longer wavelengths. This suggests that broadband absorption performance is enhanced by raising the dielectric height, particularly in the infrared spectrum.

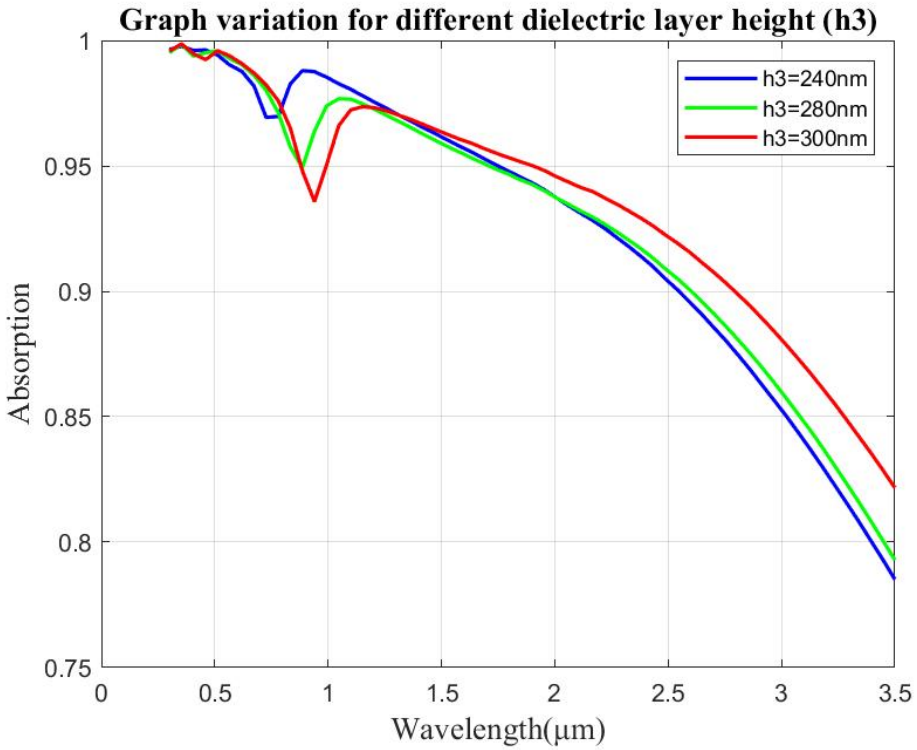

Figure 4.7: Absorption spectra for different heights of the dielectric material (h_3 = 240nm, 280 nm and 300nm), showing the impact on bandwidth and spectral response.

Increasing the dielectric layer height (h3) improves absorption at longer wavelengths and reduces the sharpness of the absorption dip near 1 μm.

4.4.6 Result Variation for Different Gold Layer Height (h_4)

The result is independent of this layer height. This is a metallic layer, working as a conductor and reflector. If any light ray is not absorbed, then this layer reflects it back to the absorbing material again to further absorb it.

4.4.7 Result Variation for Different Metal as Absorbing Material

When various metallic materials—specifically, tungsten, platinum, nickel, and titanium—are employed as the primary absorbing layer, the graph shows the absorption properties of the metasurface absorber.

Titanium (red curve) has the broadest and highest absorption of all the materials, continuously exceeding 90%, which makes it an excellent choice for ultra-wideband absorption. Although nickel (magenta) also works well in the visible spectrum, its use in broadband applications is limited because of a noticeable drop in efficiency after 1.5 µm. With a more pronounced decline in absorption in the infrared spectrum, platinum (green) exhibits moderate performance. Beyond 1.5 µm, tungsten (blue) performs the worst, with absorption dropping below 20%.

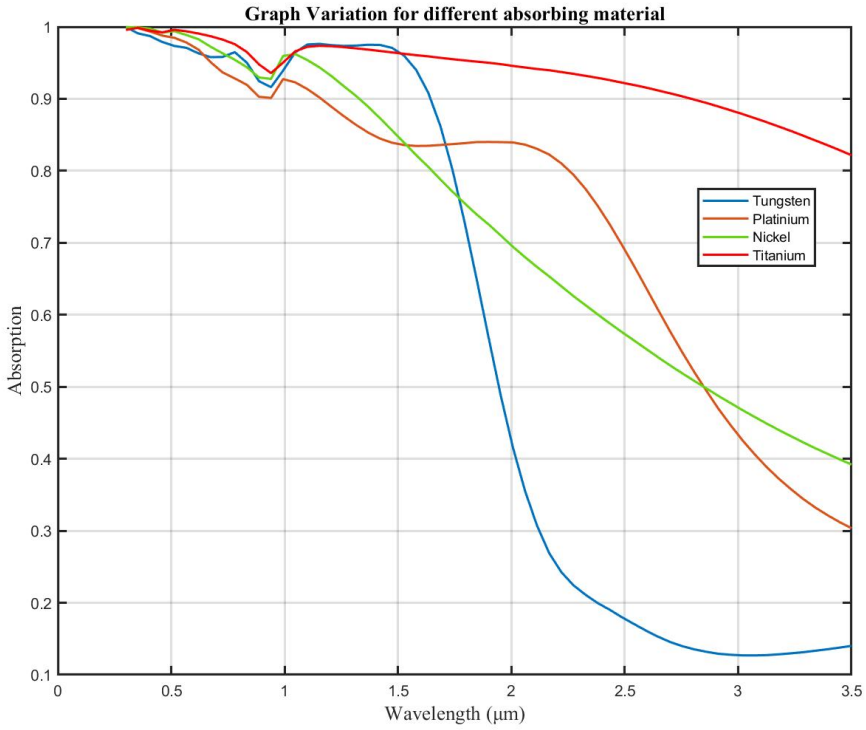

Figure 4.8: Tested different material as absorbing material and the graph presents the result.

Titanium's superior absorption makes it the most appropriate material for ultra-wideband metasurface absorber designs, according to this comparative analysis.

4.4.8 Result Variation for Different Incident Angles

Absorption versus wavelength is displayed on the graph for a range of incident angles, from 0° to 40°. In the shorter wavelength range (0.3–1 µm), all curves retain high absorption above 0.9. Around 1 µm, there is a dip in absorption, with deeper dips at lower angles (such as 0° and 10°). Absorption improves with increasing incident angle, particularly in the longer wavelength range and close to the dip. Over the majority of the spectrum, the 40° curve exhibits the highest overall absorption. All curves gradually decrease after 1.5 µm, but they still exhibit absorption above 0.75.

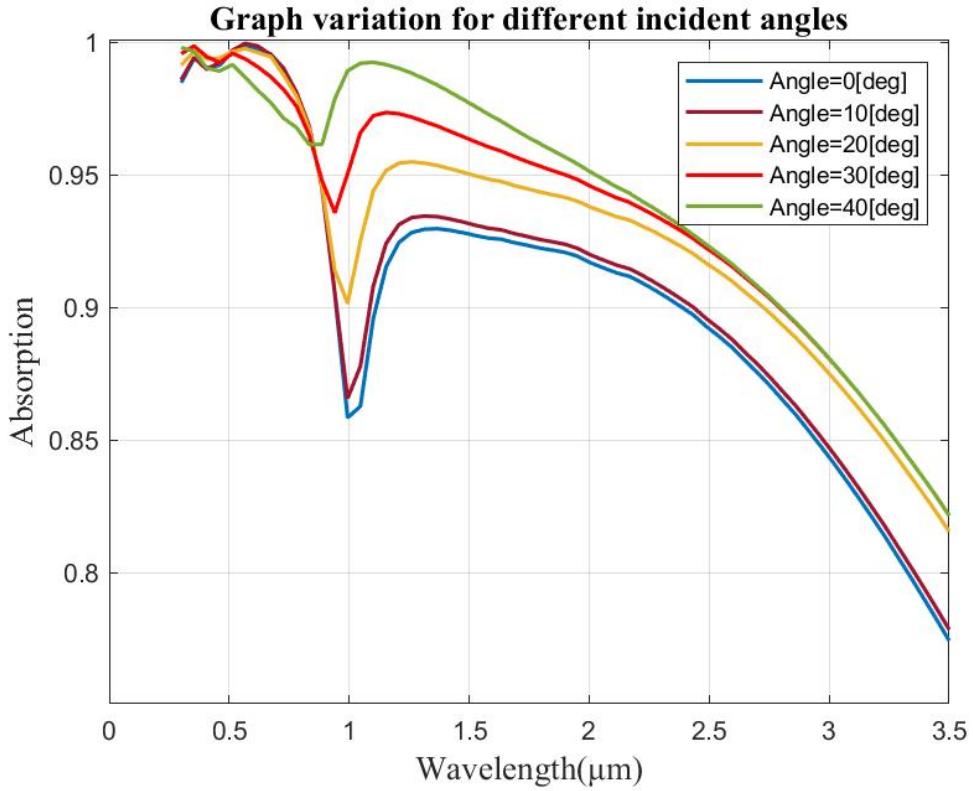

Figure 4.9: Experimented with different incident angles, and the result is presented by the figure.

Higher incident angles (30°–40°) enhance absorption, particularly at wavelengths above 1 µm and around the dip near 1 µm. The structure exhibits angular tolerance, making it suitable for broadband and wide-angle optical applications.

4.4.9 Comparison

Table 4.1: Comparison table with proposed work and previous works.

Reference	Wavelength Spectrum / Frequency Bandwidth	Absorption
[43]	Wavelength spectrum 1100 nm (from 400 nm to 1500 nm).	95.14%
[44]	Frequency bandwidth 810 THz (340 THz to 1150 THz)	92.2%
[45]	Double narrow band	96%
[22]	Around 608 THz frequency bandwidth	70%
[46]	For 2000 nm wavelength spectrum	80%
Proposed design	2500 nm wavelength spectrum (from 300nm to 2800 nm) 3200 nm wavelength spectrum (from 300nm to 3500 nm)	95.61% 93.47%

4.5 Issues Associated with Society, Health, Culture, and Practice of Professional Engineering

The creation and use of cutting-edge solar energy technologies, like ultra-wideband metasurface absorbers, have important ramifications for professional engineering, society and health.

From a societal standpoint, this study helps to reduce reliance on fossil fuels and greenhouse gas emissions while meeting the demand for clean and sustainable energy worldwide. In order to enable technologies like solar thermal systems, which are essential for rural electrification and energy access in underprivileged communities, efficient solar absorbers are essential.

The suggested design complies with environmentally friendly engineering practices in terms of health and safety since it is non-toxic and does not use radioactive or dangerous materials. It indirectly improves public health by lowering the demand for energy sources that emit pollutants, which results in better air quality and lower climate risks.

Lastly, this work adhered to professional engineering practices, which include acknowledging previous research, validating results, sourcing material data ethically, and simulating accuracy. The approach responsibly advances science and technology while adhering to international engineering standards.

4.6 Sustainability and Environmental Impact

Sustainability and environmental responsibility are fundamentally compatible with the suggested ultra-wideband metasurface-based solar absorber. It maximizes the use of a plentiful, renewable energy source without depending on fossil fuels or producing greenhouse gases by making it possible to harvest solar radiation efficiently across a wide spectrum (300–3500 nm).

In terms of sustainability, the absorber is small and makes use of titanium, a metal that is recyclable and reasonably abundant. The structure's environmentally friendly profile is further improved by the use of dielectric materials like SiO_2 which are widely accessible and non-toxic. Because of its straightforward and planar geometry, it can be produced using low-cost and scalable techniques, opening the door to possible mass production.

4.7 Discussion

According to the simulation results, the suggested ultra-wideband metasurface-based solar absorber achieves an average absorptance above 93% and operates effectively over a broad spectral range (300–3500 nm), and average absorption was abin thee 95% in 300 nm to 2800 nm spectrum. The optimized geometry and material selection, where the dielectric spacer guarantees impedance matching and the patterned titanium top layer supports plasmonic resonances, are responsible for this high performance.

Notwithstanding these encouraging results, experimental confirmation is required to address possible fabrication flaws and practical impacts. All things considered, this work shows great promise for realistic, sustainable solar energy harvesting with metasurface technology.

4.8 Summary

The design, modeling, and deployment of an ultra-wideband metasurface-based solar absorber were covered in this chapter. The absorber was modeled and optimized using COMSOL Multiphysics to attain a high absorptance (>93%) in the 300–3500 nm spectral range. The design performed well in a range of incident polarizations and angles. Details were provided on meshing, boundary conditions, material properties, and important implementation steps. The chapter also covered the absorber's practicality, sustainability advantages, and possible drawbacks, highlighting its potential for effective and expandable solar energy harvesting systems.

Chapter 5

Conclusion and Future Scopes

5.1 Introduction

The main findings of the study are outlined in this concluding chapter, along with its importance and possible future research directions. The chapter summarizes the contributions made to the design of an ultra-wideband, high-performance metasurface absorber and considers its applications.

5.2 Thesis Conclusion

The aim of this study was to design and numerically study a metasurface-based solar absorber that can absorb ultra-wideband light, i.e., visible to short-wave infrared (SWIR) light from 300 nm to 3500 nm. The study effectively illustrated a design that achieved an average absorptance of more than 93% across the desired spectral range using a patterned titanium nanostructure supported by a metallic ground plane and dielectric spacer.

The spectral response, angular and polarization tolerance, and energy confinement behavior of the absorber were investigated in detail using FEM-based simulation in COMSOL Multiphysics. It was discovered that destructive interference of reflected waves, impedance matching, and plasmonic resonance were the causes of the high absorption.

The design's straightforward geometry, thermal stability, and robust spectral performance also make it promising for practical uses in solar thermal energy harvesting, photodetectors, and infrared sensors. All things considered, this work offers a workable and expandable approach to the effective and sustainable use of solar energy.

5.3 Future Scopes

Although the absorber's potential has been demonstrated by the simulation-based investigation, there are still a number of areas that need more research:

- **Experimental Fabrication:** In order to validate simulation results, future work should physically fabricate the suggested design using thin-film deposition or nanolithography techniques, followed by optical characterization.
- **Alternative Materials:** Investigating phase-change materials or other refractory metals (such as tantalum or tungsten) may improve tunability and thermal endurance.
- **Thermal Simulation:** Heat distribution and efficiency under actual solar irradiance can be better understood by incorporating coupled thermal–optical simulations.
- **Integration in Device:**The absorber's real-time performance and commercial viability can be evaluated by integrating it into useful devices such as infrared imagers or thermophotovoltaic systems.
- **Optimization Algorithm:** By using genetic or AI-driven optimization techniques, structural dimensions can be further refined for increased efficiency or customized absorption profiles.

5.4 Summary

By highlighting the main conclusions and going over the research's wider ramifications, this chapter brought the thesis to a close. The suggested design has a lot of potential for energy technologies in the future, and the future scopes described offer a way forward for further development and useful application.

REFERENCES

[1] A. Shafique, M. A. Naveed, S. Ijaz, M. Zubair, M. Q. Mehmood, and Y. Massoud, "Highly efficient vanadium nitride based metasurface absorber/emitter for solar-thermophotovoltaic system," *Materials Today Communications*, vol. 37, p. 105416, 2023.

[2] Z. Ding, W. Su, L. Ye, W. Li, Y. Zhou, B. Tang, J. Zou, and H. Yao, "Deep learning based inverse design of metasurface absorber for maximizing solar spectral absorption," *Solar Energy*, vol. 2024, p. 112449, 2024.

[3] Y. Ye, H. Wang, X. Li, and Y. Zhao, "Omnidirectional, polarization-insensitive and broadband thin absorber in the terahertz regime," *Journal of the Optical Society of America B*, vol. 27, no. 3, pp. 498–504, 2010.

[4] Y. He *et al.*, "Plasmonic light trapping in an ultrathin photovoltaic layer with film-coupled metamaterial structures," *AIP Advances*, vol. 5, no. 2, p. 027104, 2015.

[5] Z. Ashrafi-Peyman, A. Jafargholi, and A. Z. Moshfegh, "An elliptical nanoantenna array plasmonic metasurface for efficient solar energy harvesting," *Nanoscale*, vol. 16, pp. 3591–3605, 2024.

[6] G. Hou, Z. Lin, Q. Wang, Y. Zhu, J. Xu, and K. Chen, "Integrated silicon-based spectral reshaping intermediate structures for high performance solar thermophotovoltaics," *Solar Energy*, vol. 249, pp. 227–232, 2023.

[7] A. K. Azad, W. J. M. Kort-Kamp, M. Sykora, N. R. Weisse-Bernstein, T. S. Luk, A. J. Taylor, D. A. R. Dalvit, and H.-T. Chen, "Metasurface broadband solar absorber," *arXiv preprint arXiv:1509.06666*, 2015.

[8] C. Sun *et al.*, "Metamaterial-plasmonic absorber structure for high efficiency amorphous silicon solar cells," *Nano Letters*, vol. 12, no. 1, pp. 1–7, 2012.

[9] C. Ji, K. Lee, T. Xu, J. Zhou, H. J. Park, and L. J. Guo, "Engineering light at the nanoscale: structural color filters and broadband perfect absorbers," *Advanced Optical Materials*, vol. 5, no. 20, p. 1700368, 2017.

[10] C. Luo, X. Yang, L. Wang, L. Wu, C. Liu, D. Lei, W. Wu, D. P. Tsai, and L. J. Guo, "Ultra-broadband light absorption by a sawtooth anisotropic metamaterial slab," *Optics Express*, vol. 23, no. 7, pp. 8670–8680, 2015.

[11] A. K. Osgouei, A. Ghobadi, B. Khalichi, R. A. Sabet, O. Tokel, and E. Ozbay, "Visible light metasurface for adaptive photodetection," *Journal of Physics D: Applied Physics*, vol. 55, no. 47, p. 475103, 2022.

[12] C. Wu, Y. Liu, J. Li, and X. Zhang, "Ultra-narrow band perfect absorber and its application as plasmonic sensor in the visible region," *Nanoscale Research Letters*, vol. 12, no. 1, p. 427, 2017.

[13] I. L. Rasskazov, N. Sonwalkar, and P. S. Carney, "Light scattering by plasmonic disks and holes arrays: different or the same?," *Journal of Physics D: Applied Physics*, vol. 55, no. 45, p. 455104, 2022.

[14] Y. Zhang, H. Li, X. Wang, and Y. Chen, "Improving the mid-infrared energy absorption efficiency by using a dual-band metamaterial absorber," *Progress in Natural Science: Materials International*, vol. 24, no. 2, pp. 128–132, 2014.

[15] X. Jiang, H. Yuan, D. Chen, Z. Zhang, T. Du, H. Ma, and J. Yang, "Metasurface based on inverse design for maximizing solar spectral absorption," *Advanced Optical Materials*, vol. 9, no. 19, p. 2100575, 2021.

[16] A. D. Khan, S. D. Khan, and M. Noman, "Light absorption enhancement in tri-layered composite metasurface absorber for solar cell applications," *Optical Materials*, vol. 84, pp. 195–198, 2018.

[17] M. Xu, L. Guo, P. Zhang, Y. Qiu, Q. Li, and J. Wang, "Near-perfect spectrally-selective metasurface solar absorber based on tungsten octagonal prism array," *RSC Advances*, vol. 12, pp. 16823–16834, 2022.

[18] P. P. Nakti, D. Sarker, M. I. Tahmid, and A. Zubair, “Ultra-broadband near-perfect meta-material absorber for photovoltaic applications,” *Nanoscale Advances*, vol. 5, pp. 6858–6869, 2023.

[19] W. Wang, S. Wu, Y. Liu, X. Sun, Z. Liao, D. Lei, and L. J. Guo, “Broadband and thin optical absorber based on a plasmonic nanohelix array,” *Optics Express*, vol. 28, no. 20, pp. 29927–29935, 2020.

[20] S. Kanungo, K. V. Srivastava, and S. Saha, “Broadband metamaterial absorber for visible to near infrared region,” *Optical Materials*, vol. 100, p. 109400, 2020.

[21] U. Solanki and P. Mandal, “Phase sensitive vo2-metal switchable plasmonic metasurface for thermal controlling of broad band near-infrared absorption,” *Optical and Quantum Electronics*, vol. 54, no. 12, pp. 1–14, 2022.

[22] Y. Bai, L. Zhao, D. Ju, Y. Jiang, and L. Liu, “Wide-angle, polarization-independent and dual-band infrared perfect absorber based on l-shaped metamaterial,” *Optics Express*, vol. 23, pp. 8670–8680, Apr. 2015.

[23] P. Q. Yu, Y. Wang, X. Zhang, and H. Li, “Broadband metamaterial absorbers,” *Advanced Optical Materials*, vol. 7, no. 1, p. 1800995, 2019.

[24] A. Dhawan *et al.*, “Anti-reflective graded-index metasurface with correlated disorder for light management in planar silicon solar cells,” *Advanced Optical Materials*, vol. 12, no. 3, p. 2302964, 2024.

[25] A. Armghan, M. Alsharari, M. A. Baqir, M. Saqlain, and K. Aliqab, “A high-performance ultra-wideband metasurface absorber and thermal emitter for solar energy harvesting and thermal applications,” *Physical Chemistry Chemical Physics*, vol. 26, pp. 25469–25479, 2024.

[26] C. R. Simovski, D. K. Morits, P. M. Voroshilov, M. E. Guzhva, P. A. Belov, and Y. S. Kivshar, “Enhanced efficiency of light-trapping nanoantenna arrays for thin film solar cells,” *arXiv preprint arXiv:1301.3290*, 2013.

[27] M. D. E. Karim and A. S. M. Mohsin, “Metasurface absorber based single junction thin film solar cell exceeding 30% efficiency,” *Optics Express*, vol. 32, no. 5, pp. 8214–8225, 2024.

[28] R. A. Pala, S. Butun, K. Aydin, and H. A. Atwater, "Omnidirectional and broadband absorption enhancement from trapezoidal mie resonators in semiconductor metasurfaces," *arXiv preprint arXiv:1512.04305*, 2015.

[29] Z. Yu, A. Raman, and S. Fan, "Fundamental limit of nanophotonic light-trapping in solar cells," *arXiv preprint arXiv:1004.2902*, 2010.

[30] X. Lu, Y. Liu, J. Zhang, and W. Zhu, "Tunable near-perfect light absorber consisted of gold cylinder and phase changing material in the near-infrared regime," *Indian Journal of Physics*, vol. 96, no. 4, pp. 549–556, 2022.

[31] N. I. Landy, S. Sajuyigbe, and J. J. Mock, "Perfect metamaterial absorber," *Physical Review Letters*, vol. 100, p. 207402, 2008.

[32] J. K. Li, X. F. Chen, Z. Yi, H. Yang, Y. J. Tang, Y. Yi, W. T. Yao, J. Q. Wang, and Y. G. Yi, "Broadband solar energy absorber based on monolayer molybdenum disulfide using tungsten elliptical arrays," *Materials Today Energy*, vol. 16, p. 100390, 2020.

[33] L. Hao, Q. Li, K. K. Du, Z. Q. Xu, H. Z. Zhu, D. L. Liu, L. Cai, P. Ghosh, and M. Qiu, "An ultra-thin colored textile with simultaneous solar and passive heating abilities," *Nano Energy*, vol. 65, p. 103998, 2019.

[34] Y. Cheng and C. Du, "Broadband plasmonic absorber based on all silicon nanostructure resonators in visible region," *Optical Materials*, vol. 98, p. 109441, 2019.

[35] F. Qin, Z. Q. Chen, X. F. Chen, Z. Yi, W. T. Yao, T. Duan, P. H. Wu, H. Yang, G. F. Li, and Y. G. Yi, "A tunable triple-band near-infrared metamaterial absorber based on au nano-cuboids array," *Nanomaterials*, vol. 10, no. 2, p. 207, 2020.

[36] Y. Y. Wang, Z. Q. Chen, D. Y. Xu, Z. Yi, X. F. Chen, J. Chen, Y. J. Tang, P. H. Wu, G. F. Li, and Y. G. Yi, "Triple-band perfect metamaterial absorber with good operating angle polarization tolerance based on split ring arrays," *Results in Physics*, vol. 16, p. 102951, 2020.

[37] M. Y. Pan, Y. Huang, Q. Li, H. Luo, H. Z. Zhu, S. Kaur, and M. Qiu, "Multi-band middle infrared-compatible camouflage with thermal management via simple photonic structures," *Nano Energy*, vol. 69, p. 104449, 2020.

[38] S. K. Agnihotri, D. V. Prashant, and D. P. Samajdar, "Role of metallic nanoparticles in the optoelectronic performance enhancement of inp ultrathin film solar cell," *Optical Materials*, vol. 134, p. 113129, 2022.

[39] C. Sun, H. Liu, B. Yang, K. Zhang, B. Zhang, and X. Wu, "An ultra-broadband and wide-angle absorber based on a tin metamaterial for solar harvesting," *Physical Chemistry Chemical Physics*, vol. 25, no. 1, pp. 806–812, 2022.

[40] X. Kong, S. Jiang, L. Kong, Q. Wang, H. Hu, X. Zhang, and X. Zhao, "Transparent metamaterial absorber with broadband rcs reduction for solar arrays," *arXiv preprint arXiv:2003.13005*, 2020.

[41] A. S. Rana, "Tungsten based metasurface absorber for visible regime," *arXiv preprint arXiv:1708.04438*, 2017.

[42] A. Shafique, M. A. Naveed, S. Ijaz, M. Zubair, M. Q. Mehmood, and Y. Massoud, "Highly efficient vanadium nitride based metasurface absorber/emitter for solar-thermophotovoltaic system," *Materials Today Communications*, vol. 35, p. 105416, 2023.

[43] M. Kumar, D. K. Dwivedi, A. Kumar, and R. K. Sinha, "Highly sensitive and selective sensor based on photonic crystal waveguide with ring resonator," *Optics Express*, vol. 28, pp. 28152–28163, Sept. 2020.

[44] R. Ahmad, S. K. Jha, and S. Singh, "Simulation of photonic crystal based ring resonator for gas sensing application," *Physica B: Condensed Matter*, vol. 596, p. 412503, Sept. 2020.

[45] K. Lee, J.-H. Lee, Y.-S. Kim, S.-H. Han, and B. Kim, "Light absorption enhancement in tri-layered composite metasurface absorber," *Optical Materials*, vol. 84, pp. 195–202, Sept. 2018.

[46] P. Yu, H. Yang, X. Chen, Z. Yi, W. Yao, J. Chen, Y. Yi, and P. Wu, "Ultra-wideband solar absorber based on refractory titanium metal," *Renewable Energy*, vol. 158, pp. 227–235, Oct. 2020.